Biosensors and Bioelectronics 71 (2015) 75–81

Contents lists available at ScienceDirect

Biosensors and Bioelectronics

journal homepage: www.elsevier.com/locate/bios

Electrochemical plasmonic sensing system for highly selective multiplexed detection of biomolecules based on redox nanoswitches

Anne-Marie Dallaire [a], Sergiy Patskovsky [a], Alexis Vallée-Bélisle [b,*], Michel Meunier [a,**]

[a] Laser Processing and Plasmonics Laboratory, École Polytechnique de Montréal, Department of Engineering Physics, C.P. 6079, succ. Centre-Ville, Montréal, QC, Canada H3C 3A7

[b] Laboratory of Biosensors and Nanomachines, Université de Montréal, Department of Chemistry, C.P. 6128, succ. Centre-Ville, Montréal, QC, Canada H3C 3J7

ARTICLE INFO

Article history:
Received 5 February 2015
Received in revised form
24 March 2015
Available online 7 April 2015

Keywords:
Surface plasmon resonance
Structure-switching biosensor
Electrochemistry
Nanosensors

ABSTRACT

In this paper, we present the development of a nanoswitch-based electrochemical surface plasmon resonance (eSPR) transducer for the multiplexed and selective detection of DNA and other biomolecules directly in complex media. To do so, we designed an experimental set-up for the synchronized measurements of electrochemical and electro-plasmonic responses to the activation of multiple electrochemically labeled structure-switching biosensors. As a proof of principle, we adapted this strategy for the detection of DNA sequences that are diagnostic of two pathogens (drug-resistant tuberculosis and *Escherichia coli*) by using methylene blue-labeled structure-switching DNA stem-loop. The experimental sensitivity of the switch-based eSPR sensor is estimated at 5 nM and target detection is achieved within minutes. Each sensor is reusable several times with a simple 8 M urea washing procedure. We then demonstrated the selectivity and multiplexed ability of these switch-based eSPR by simultaneously detecting two different DNA sequences. We discuss the advantages of the proposed eSPR approach for the development of highly selective sensor devices for the rapid and reliable detection of multiple molecular markers in complex samples.

1. Introduction

Faster advancement of biosensor technologies for point-of-care applications requires the development of devices that are sensitive, portable, reliable and, most importantly, sufficiently selective to work directly in complex media (Rosi and Mirkin, 2005). Potential solutions for the improvement of existing biosensing methods can originate either from new advancements in technologies or from the combination of well-established approaches that will mutually contribute to the quantity and quality of required analytical parameters. Notable examples of the later strategy are the combination of quartz crystal microbalance and surface plasmon resonance (SPR) (Reimhult et al., 2004), dielectrophoresis and nanoplasmonic (Barik et al., 2014) and not the least SPR and electrochemistry (Dahlin et al., 2012a; Sannomiya et al., 2010; Wang et al., 2011).

It has early been established that the application of an electrical potential affects the properties of surface plasmons (Gordon and Ernst, 1980; Koetz et al., 1977), however the mechanisms behind this effect are still not completely understood (Dahlin et al., 2012b). The major contributions have been identified as variations in the electron density at the metal surface, changes in the double layer capacitance, electrochemical formation of an interfacial thin film, and changes in bulk refractive index often induced by redox reactions (Wang et al., 2010). The experimental combination of electrochemical and surface plasmon resonance sensing (eSPR) is inherently simple as it only requires a sensing surface that is both conductive and plasmonic (e.g. the conventional gold SPR chip). This technique has been successfully used in a wide range of applications such as thin films characterization (Baba et al., 2004), the study of redox reactions at a metal/liquid interface (Iwasaki et al., 1998; Wain et al., 2008) and biosensing (Kang et al., 2001; Nakamoto et al., 2012; Patskovsky et al., 2014). One of its main advantages for biosensing is that eSPR is less sensitive to bulk refractive index changes and non-specific adsorption than conventional SPR (Lu et al., 2012). In recent years, the Tao group has combined electrochemistry with imaging SPR, achieving high resolution mapping of electrochemical phenomena with a sensitivity that is not obtainable by either method on their own (MacGriff et al., 2013; Shan et al., 2010; Wang et al., 2011), underlining the potential for eSPR as a multi-parametric analytical technique with enhanced performance.

In this paper, we report the development of a new sensing

* Corresponding author.
** Corresponding author. Fax: +1 514 340 5195.
E-mail addresses: a.vallee-belisle@umontreal.ca (A. Vallée-Bélisle), michel.meunier@polymtl.ca (M. Meunier).

http://dx.doi.org/10.1016/j.bios.2015.04.011
0956-5663/

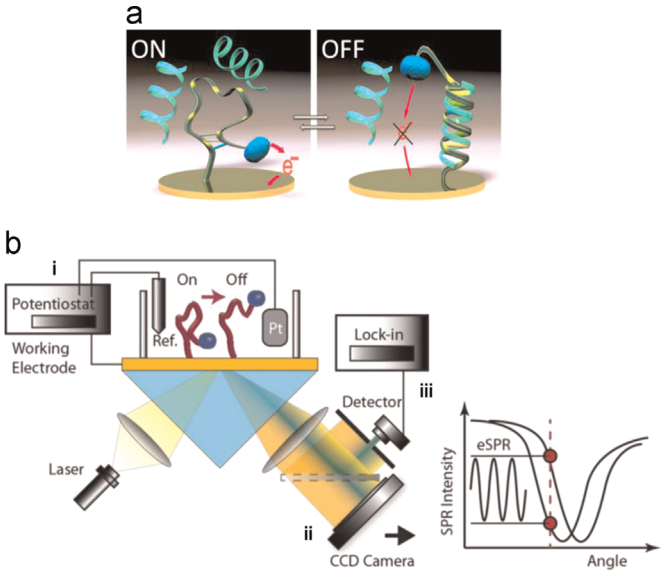

Fig. 1. (a) Schematic of the nanoswitches signalization mechanism. When the target binds the immobilized probe, the switch undergoes a conformational change from the "ON" state to the "OFF" state that increases the distance between the methylene blue reporter (blue sphere) and the electrode, hindering the electron transfer process. (b) Schematic of the multi-parametric plasmonic biosensor for the detection of oligonucleotides assisted with electrochemical nanoswitches. A potentiostat is used to measure electrochemical voltammograms (i) and apply the voltage on the gold surface. The light containing plasmonic information is collected in two ways. First, a collimated beam is detected on a CCD camera to obtain the full angular/intensity dependency used in conventional angular SPR sensing (ii). Second, light from a fixed angle is sent on a photodetector. The average intensity measured by this Si detector is the SPR curve intensity at fixed angle (DC component). The detector is also coupled to a lock-in amplifier to obtain the eSPR signal (AC component) (iii). The inset graph shows the relation between the full SPR curve and the eSPR signal as the refractive index is modulated. (For interpretation of the references to color in this figure legend, the reader is referred to the web version of this article.)

device that combines the sensitivity and multiplexing capability of eSPR methods together with the selectivity and robustness of structure-switching sensors (Lubin and Plaxco, 2010; Vallee-Belisle and Plaxco, 2010). We expect this combined approach to improve the selectivity of plasmonic sensing in complex media and to have more multiplexing potential than electrochemical sensors.

As a proof of principle model for our eSPR transducer, we first adapted the well-characterized E-DNA sensor "nanoswitch", which consists in a DNA stem-loop (Fan et al., 2003) that contains an electroactive reporter (e.g. methylene blue MB) at one of its extremity and a thiol group at the other extremity to promote immobilization to the electrode surface (Fig. 1a). Upon binding of its complementary DNA sequence or target biomolecule on the loop, this stem-loop undergoes stem opening, which separates the electroactive reporter from the electrode surface, leading to a significant decrease in the electron transfer rate, thus affecting the measurable electrochemical signal. As the conformational changes of the structure-switching probe only occurs upon binding of the specific target, the measured signal is mostly unaffected by non-specific adsorption of contaminant molecules on the sensor head. In this article we designed and tested a multiplexed eSPR switch sensing device and obtained preliminary experimental results for DNA detection in whole blood, confirming the good potential of the structure-switching sensor for a reliable biosensing in complex samples such as bodily fluids or foodstuffs.

2. Materials and methods

2.1. Materials

Labeled oligonucleotide nanoswitches were purchased from Biosearch Technologies (Petaluma, CA). Two oligonucleotide nanoswitches were designed and synthetized: Nanoswitch_1: 5′ HS-C6- act ctc caa gcg ccg act gtt gag agg -MB 3′ and Nanoswitch_2: 5′ HS-C6- act ctc gat cgg cgt tt ta gag agg -MB 3′, the first which contains a sequence that is complementary to the rpoB gene of *Mycobacterium Tuberculosis* associated with drug resistant tuberculosis (Rachkov et al., 2011), the second with a sequence associated to *Escherichia coli*. Both sequences are modified on their 5′ extremity with a hexamethylene linker (C6) and a thiol group to promote immobilization to the gold surface and on their 3′ extremity with a methylene blue (MB) redox reporter. Both nanoswitches were designed in a stem-loop conformation with a 5 base pair stem that contains 4 GC and 1 AT to insure sufficient stem stability. Oligonucleotides Target_1 (5′ tc aa cag tcg gcg ctt gg 3′) and Target_2 (5′ ctc ta aa acg ccg atc gag 3′) were designed to be complementary to Nanoswitch_1 and Nanoswitch_2. Bovine whole blood was purchased from Innovative Research Inc. All other reagents were obtained from Sigma-Aldrich.

2.2. Sensor preparation

To fabricate the sensing chips, a 5 nm chromium adhesion layer and a 50 nm gold layer were deposited on BK7 glass slides using an electron beam evaporator. Prior to functionalization, slides were cut into smaller 1 cm^2 chips, cleaned in a fresh "piranha" solution (H_2SO_4 3:1 H_2O_2) (WARNING: Piranha solution is highly hazardous, handle with care in a fume hood and avoid contact with organic matter), rinsed abundantly in MilliQ water and dried under a N_2 flow. The nanoswitches were immobilized on the sensor surface using thiol-gold chemistry according to the following protocol (Rowe et al., 2011). To reduce disulfide bonds between the thiol-modified nanoswitches, 2 μL of 100 μM nanoswitches were incubated with 4 μL of 10 mM tris(2-carboxyethyl)phosphine (TCEP) for one hour at 4 °C. This mixture was then diluted with 300 μL of 10 mM phosphate buffered saline (pH 7.2) to obtain a final concentration of 650 nM nanoswitches. A 200 μL drop of this solution was then deposited on the gold chip and left to incubate for one hour in a humidity chamber consisting of a closed container half-filled with water. The chip was then rinsed with water and incubated in a solution of 2 mM 6-mercapto-1-hexanol (MCH) in PBS at 4 °C overnight. MCH is used as a diluent thiol to fill the free sites on the gold and has three main functions: block the surface from non-specific adsorption, prevent the oligonucleotide probes from lying on the surface (Arinaga et al., 2006) and passivate the electrode. Before the measurements, the chip was rinsed with water and let to equilibrate in PBS for 10 min. Control samples were prepared by incubating freshly cleaned gold chips in a 2 mM MCH solution overnight at 4 °C. These control samples resulted in a MCH self-assembled monolayer without nanoswitches.

The *dose–response curves* for individual sensors were obtained by sequentially increasing the target DNA concentration. Dose–response curves were fitted to a single-site binding mechanism ($[T]$=target concentration; Amp=Maximum signal attenuation; $C_{50\%}$=concentration of target at which 50% of the sensor's signaling amplitude is reached):

$$\text{Signal attenuation}_{[T]} = \text{Amp}\ [T]/([T]+C_{50\%})$$

2.3. Experimental set-up

We designed the multi-parametric experimental platform

presented in Fig. 1b to perform our synchronous measurements of electrochemical voltammograms, conventional angular SPR dependencies and eSPR signal. A 633 nm laser light source (CrystalLaser), convergence optics and a BK7 coupling prism were used for SPR excitation over a 50 nm surface plasmon supporting gold film in the Kretschmann configuration. The same metal film was used as a working electrode in electrochemical experiments controlled by a ModuLab potentiostat in a three-electrode configuration. The working area of the gold metal film was a 3 mm diameter disk. We used a larger 1 cm platinum disk as a counter-electrode and an Ag/AgCl electrode filled with 3 M KCl electrolyte as a reference. The reference electrode was positioned 2 mm from the working electrode. Upon application of a voltage modulation on the gold film, SPR at a fixed angle generated an electro-optical response (eSPR), which was measured by an amplified Si detector (Thorlabs) connected to a lock-in amplifier (SR830, Stanford Research Systems) (Fig. 1b iii). The signal measured by this detector contains two parameters: the average "DC" SPR intensity at a fixed angle, and the "AC" amplitude upon modulation of the refractive index (i.e. the eSPR amplitude, in mV). A teflon measuring open-cell with a capacity of 5 mL was designed and the liquid was agitated at constant speed with a stirrer (Instech) during experiments.

3. Results and discussions

3.1. Espr structure switching sensor

The principle behind eSPR sensing relies on the optical detection of the nanoswitches' MB tags redox reaction (Fig. 2a). In its initial state, the sensor is covered with nanoswitches in their folded "ON" configuration where their MB group is fixed near the surface. When the potential on the gold surface is swept towards negative values, the MB may gain electrons from the electrode and be reduced to MB_{red}. When the potential is swept towards positive values, MB_{red} may lose electrons to the electrode and be oxidized to MB_{ox}. Since MB_{red} and MB_{ox} have different refractive indices (RI), what will be sensed by the SPR is a thin layer with an effective refractive index RI_{redON} (at very negative potential) or RI_{oxON} (at less negative potential), with a difference of $\Delta RI_{redoxON}$. When the target binds the nanoswitch, it unfolds to its "OFF" configuration where the MB is brought far from the surface. As the electron transfer rate is highly dependent on the distance to the electrode, less MB molecules will be oxidized and reduced when the potential is swept, and the difference between RI_{oxOFF} and RI_{redOFF} sensed by SPR will be the lower $\Delta RI_{redoxOFF}$. Therefore, the target can be detected through a measurement of ΔRI_{redox}.

In order to measure ΔRI_{redox} with eSPR, gold samples were functionalized with Nanoswitch_1 and MCH using the protocol from Section 2.2. We monitored the immobilization step with angular SPR which resulted in an average shift of $2.3 \times 10^{-3} \pm 7\%$ RIU. Using the Maxwell–Garnett effective medium theory and parameters described in (Dallaire et al., 2012), we estimated the filling factor of Nanoswitch_1 to be 22% corresponding to a surface coverage of 5.8×10^{12} nanoswitches/cm^2. As a control, a second sample was prepared with only MCH.

The first eSPR method tested was to run cyclic potential sweeps in PBS (0 to −450 mV, 10 mV/s) on each sample and to measure the resulting shift in refractive index with angular SPR (Fig. 2b).

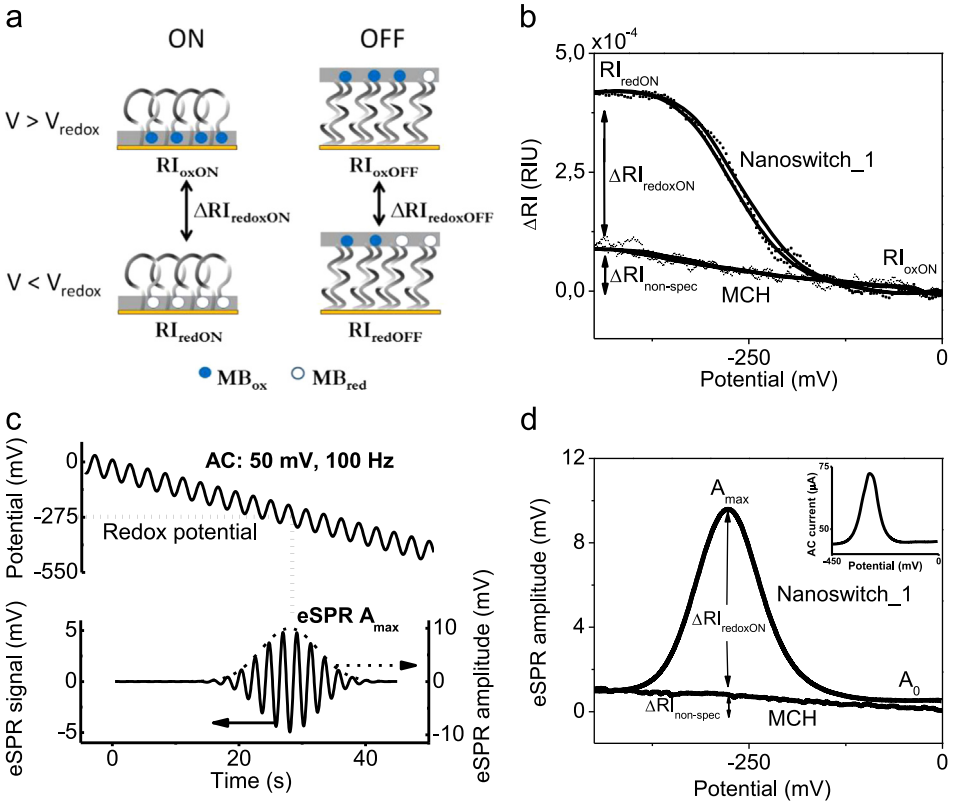

Fig. 2. (a) Schematic of the nanoswitches detection based on the refractive index (RI) changes of the methylene blue (MB) layer. Depending on the ON/OFF state of the switches, more or less MB will be oxidized and reduced as the potential V is swept across the reduction potential V_{redox}. The effective refractive index variation ΔRI_{redox} will therefore be high in the ON state and low in the OFF state. (b) Refractive index changes induced by a potential sweep on a Nanoswitch_1-modified surface in its ON state (i.e. without target) and on a MCH-modified sample. (c) Schematic of the eSPR AC voltammetry methodology showing the potential applied to the surface (up) and the resulting eSPR signal and amplitude (down). (d) eSPR AC voltammograms measured experimentally for a Nanoswitch_1-modified surface and a MCH-modified surface. For comparison, an electrochemical voltammogram obtained from the same Nanoswitch_1 modified surface is shown (inset).

The MCH-modified sample showed a reversible linear increase in refractive index when the potential was swept towards negative values. As there are no MB reporters and therefore no redox reaction, this response is mostly due to the double layer capacitance and other non-specific effects ($\Delta RI_{non\text{-}spec}$). On the other hand, the Nanoswitch_1 sample showed a sigmoidal response with maximum slope at −275 mV, the redox potential of MB, as the RI reversibly changes from RI_{oxON} to RI_{redON} when the MB molecules are oxidized and reduced. The $\Delta RI_{redoxON}$ is the difference between the two samples responses and estimated at 3.3×10^{-4} RIU.

However, using this eSPR approach shows no great advantage in comparison with conventional SPR as a control MCH sample is needed to separate the contributions from ΔRI_{redox} and $\Delta RI_{non\text{-}spec}$. Nanoswitches are typically detected in the literature using square wave voltammetry, which is much more efficient at distinguishing reactions with different rates and discarding the non-specific double layer charging current (White and Plaxco, 2010). In this article, we have instead used the similar AC voltammetry technique for its ease of filtering with a lock-in amplifier.

Briefly, this eSPR method consists in applying a sinusoidal perturbation (50 mV, 100 Hz) that will rapidly oxidize and reduce the MB molecules, effectively modulating the refractive index and eSPR signal. This perturbation is superimposed on a linear sweep of potential (0 mV to −450 mV) that results in a peak of the eSPR amplitude around −275 mV typical of the redox activity of MB (Fig. 2c). The amplitude of this peak can be correlated with the electron transfer efficiency between MB and the electrode.

On Fig. 2d, we show eSPR voltammograms that were obtained experimentally for a Nanoswitch_1-modified surface and for a surface with only a MCH self-assembled monolayer. The MCH sample shows a linear voltammogram of low amplitude A_0, characteristic of double-layer capacitance. This low signal is expected as MCH passivates the electrode and prevents redox species in solution to reach the surface (Andersson et al., 2008; Shan et al., 2011). The Nanoswitch_1 sample shows two characteristics: at −275 mV, a peak of amplitude A_{max} associated with the redox activity of MB, and at 0 and −450 mV (i.e. far from the reduction potential), a line of amplitude A_0. This result indicates that the eSPR redox peak A_{max} can be normalized in regards to the background line A_0 to separate the selective amplitude response $A = A_{max} - A_0$. We confirmed that the eSPR peak originates from the redox reaction by comparing with the AC voltammogram obtained with the potentiostat (Fig. 2d inset). Indeed, electrochemical SPR is efficient at reproducing the results obtained with most conventional electrochemical methods, as was already demonstrated by the Tao group (Liang et al., 2014; Lu et al., 2012; Shan et al., 2010, 2011; Wang et al., 2010, 2011).

We first tested the performance of our eSPR structure-switching sensor by detecting a single stranded DNA sequence in PBS buffer. Using our experimental set-up, we performed synchronous electrochemical and eSPR AC voltammetry measurement of our Nanoswitch_1-functionalized sensor following the addition of various concentrations (0.1–1500 nM) of complementary Target_1. Each target concentration was incubated with the sensing chip for 30 min before acquisition of the voltammogram. This experiment

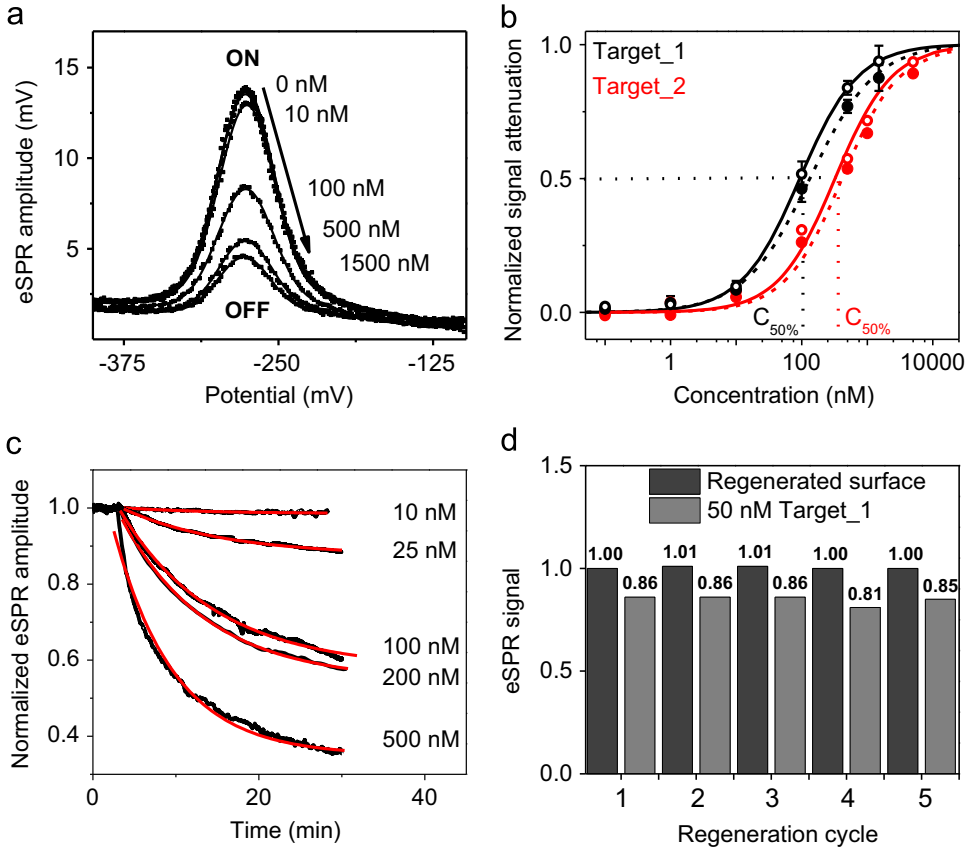

Fig. 3. Nanoswitches activation by complementary oligonucleotides. (a) eSPR AC voltammograms of a sensor functionalized with Nanoswitch_1 for different Target_1 concentrations. As the target concentration is increased, the switches are turned off and the amplitude of the eSPR redox peak decreases. (b) Dose–response curves for the Nanoswitch_1-functionalized sensor with Target_1 (black) and for the Nanoswitch_2-functionalized sensor with Target_2 (red). Responses observed with eSPR (circles, solid line) and electrochemistry (filled circles, dashed line) were concordant. All responses were measured using AC cyclic voltammetry (50 mV, 100 Hz) and normalized in relation to their maximum attenuation. (c) Real-time hybridization dynamics for various concentrations of Target_1 obtained with an eSPR impedance method (black). The kinetics were fitted with decaying exponential (red). (d) Regeneration of the sensor surface with 8 M urea. (For interpretation of the references to color in this figure legend, the reader is referred to the web version of this article.)

was repeated on three different samples. We found the eSPR voltammograms for different concentrations of target (Fig. 3a) to be almost identical to those monitored with electrochemical method (not shown). The dose–response curves for both eSPR (black circles) and electrochemical (filled black circles) were traced on Fig. 3b. As a control, we added up to 1500 nM of a mismatched oligonucleotide sequence (Target_2) and found no significant signal variation. The experience was repeated to obtain the dose–response curves for the Nanoswitch_2-functionalized sensor using Target_2 (Fig. 3b) and again eSPR (red circles) and electrochemical (filled red circles) measurements were concordant.

The noise of the sensor was defined as the standard deviation (SD) over 10 consecutive measurements of the peak amplitude of eSPR AC voltammogram in the blank sample PBS. The limit of detection was set at 3xSD and was 5 nM for Target_1 and 10 nM for Target_2. The half-signal attenuation concentrations $C_{50\%}$ measured with eSPR and electrochemistry were respectively 95 and 135 nM for Target_1 and 320 nM and 420 nM for Target_2.

We also estimated the binding kinetics of the sensor using an impedance method (DC: −275 mV, AC: 50 mV 100 Hz). The kinetics of the Nanoswitch_1/Target_1 hybridization were well fitted with an exponential decay function with lifetime τ (i.e. signal is attenuated to $1/e$) of 11 ± 1 min on average (Fig. 3c). Finally, the sensors were reusable by regenerating them in 8 M urea solution for 5 min (Fig. 3d). These results confirmed the efficiency of the eSPR approach to monitor the nanoswitch conformational changes.

3.2. Measurements in whole blood

Electrochemical structure-switching sensors have proven to be more effective than SPR label-free method for biosensing in complex samples such as blood plasma and foodstuffs (Lubin et al., 2006; Swensen et al., 2009; Vallee-Belisle and Plaxco, 2010). This is due to the fact that structure-switching mechanisms requires a significant input in energy (> 3 kcal/mol (Vallee-Belisle et al., 2009)) via a very specific binding event in order to be activated. This highly specific binding energy input (loop binding, which triggers stem opening in the case of E-DNA) cannot generally be provided by non-specific absorption on the sensor head. We therefore tested the performance of our switch-based eSPR sensor directly in whole blood. For these tests, we functionalized the gold surface with MB-containing Nanoswitch_2. We first measured the blank eSPR voltammogram in PBS, then added 200 nM of Target_2. The target was incubated for 40 min before measurement of the response eSPR voltammogram (Fig. 4a, black). During incubation, real-time hybridization dynamics were obtained with impedance method by fixing the potential at −275 mV and applying a small 50 mV perturbation at 100 Hz (Fig. 4b, black). These parameters were found suitable after analysis of the Bode plot and fitting with the equivalent circuit presented in (Uzawa et al., 2010). The sensor was then regenerated using the 8 M urea washing procedure, and the test was repeated using whole blood as a blank media (Fig. 4a and b red). The signal attenuation compared to blank values was of 43% in buffer and 46% in whole blood. They displayed similar response time in both media with $1/e$ signal decrease taking place within 11.5 min (Fig. 4b). In contrast, the angular SPR generated a very high response in the whole blood media and no clear dynamics could be observed upon addition of the target (not shown). These results confirm that electrochemical structure-switching plasmonic sensing displays a high selectivity in complex media such as bodily fluids and may be of great potential for point-of-care applications. However, it should be noted that due to the high refractive index difference between PBS and whole blood ($\Delta RI \sim 6 \times 10^{-2}$ RIU), the sensor needs to be calibrated in each media before the test (see Section 3.4).

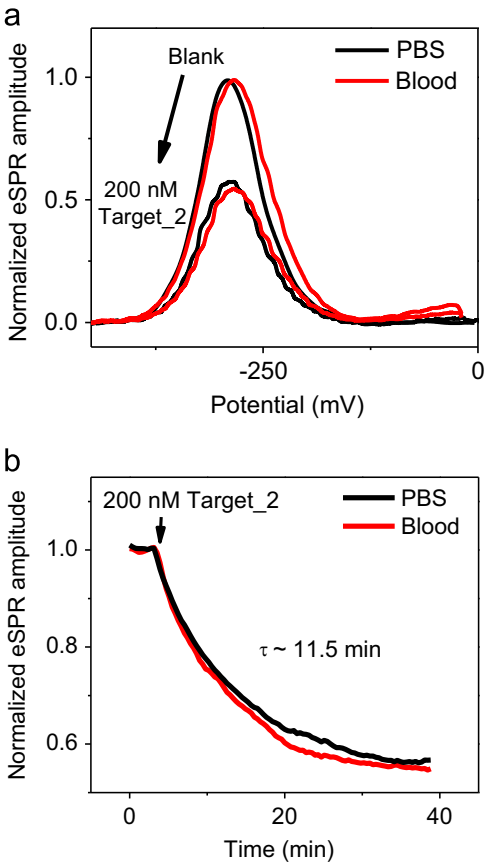

Fig. 4. (a) Normalized eSPR voltammograms of a Nanoswitch_2-modified gold surface in PBS and whole blood media. Voltammograms were acquired before and after 40 min incubation with the target oligonucleotide Target_2. (b) Real-time eSPR dynamics of hybridization between Nanoswitch_2 and Target_2. (For interpretation of the references to color in this figure, the reader is referred to the web version of this article.)

3.3. Multiplexing and differential measurements

An important advantage of the SPR methods is that the optical excitation of surface plasmons facilitates highly multiplexed detection in an array format (Scarano et al., 2010). Indeed, while electrochemistry offers no spatial resolution and is limited to measuring all the current flowing through the electrode, eSPR has the ability to map the redox potential amplitude with high spatial resolution, allowing for multi-sensing and even imaging (Shan et al., 2010). As a proof of principle for multi-detection, here we present results for the simultaneous detection of two target oligonucleotides Target_1 and Target_2 by using complementary nanoswitches Nanoswitch_1 and Nanoswitch_2 attached to the same working electrode. In this experiment, SPR reflection from two illuminated spots functionalized with Nanoswitch_1 and Nanoswitch_2 is detected by two silicon detectors connected to the inputs of a lock-in amplifier (Fig. 5a). As shown on the set-up schematic, we used a planar geometry of counter and reference electrodes that greatly facilitate sensor application in the portable format with microfluidic liquid delivery (Swensen et al., 2009). To facilitate the alignment of the double-beam for surface plasmon excitation, a BK7 dove prism was used for coupling. Using this experimental setup, we monitored in real time the successive addition of Target_1 and Target_2 using a single functionalized working electrode (Fig. 5b). By introducing 1D or 2D translation of the excitation beam we can therefore map multiplexed-electrodes where independent sensor density will be limited only by the surface plasmon propagation length or precision of DNA surface functionalization.

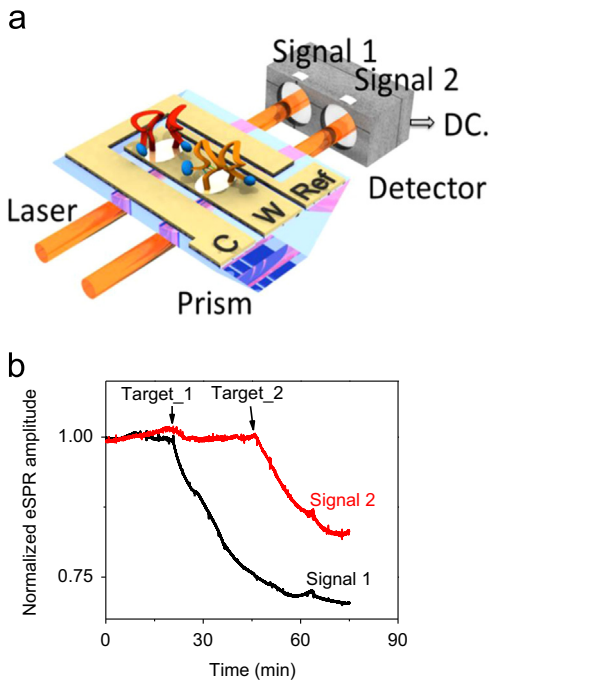

Fig. 5. (a) Multiplexed eSPR set-up. Nanoswitch_1 and Nanoswitch_2 are immobilized on two separated spots of the same working electrode immersed in the same liquid sample. (b) 100 nM Target_1 and Target_2 are subsequently added to the testing media.

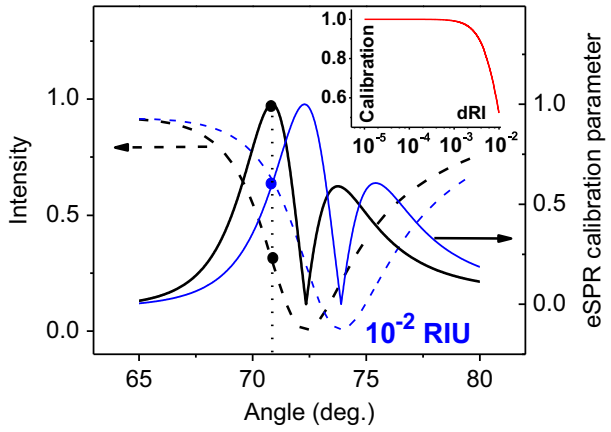

Fig. 6. Theoretical SPR angular intensity dependences (dashed) for 50 nm gold film in a water medium (black line) and shifted by 10^{-2} RIU changes (blue line). Solid lines provide the eSPR calibration parameter that corresponds to the normalized SPR curve derivative. As eSPR is measured at a fixed incident angle (dotted line), the eSPR amplitude will be affected by the bulk RI. Inset: Calibration parameter dependence on the bulk RI. (For interpretation of the references to color in this figure legend, the reader is referred to the web version of this article.)

3.4. eSPR calibration and effect of non-specific interactions

As the eSPR method is based on a modulation of the SPR intensity at fixed angle, the eSPR amplitude is proportional to the differential of the angular SPR curve (Fig. 6). Therefore, the eSPR maximum sensitivity will be achieved when measuring at the angle of maximum deviation point of the SPR dependence. However, since the differential of the SPR curve is not constant along the curve, any phenomenon that changes the experimental angle of incidence or leads to the shift of resonance curve will influence the sensor response. This is why we define the eSPR calibration parameter, which is the relative amplitude of the eSPR signal at a given angle/RI shift compared to the maximum sensitivity point. It is used to correct the effect of changes in RI to the eSPR amplitude and is directly obtained from the normalized derivative of the SPR peak. While it is very important to finely tune SPR angle at the start of experiments to the maximum sensitivity point, we observed that bulk refractive index changes up to 10^{-3} RIU had a calibration parameter >0.99 which did not considerably affect the eSPR signal (Fig. 6 inset). We tested with conventional SPR that hybridization of saturating concentrations of target molecules in buffer resulted in RI changes 10^{-3} RIU, and therefore did not need to be corrected. In some cases, it is however necessary to eliminate possible error linked to the formation of a nonspecific thin film at the surface of the sensor or by a change in the bulk refractive index of the sample. To do so, we tested three methods. Using the full SPR curve measured with conventional angular SPR, we measured the resonant angle shift between the blank and after hybridization of the target, then recalculated the eSPR calibration parameter. A second approach consisted in repeatedly readjusting the incident angle at the maximum deviation point of the SPR curve. Although it requires a complicated experimental set-up, the later method was needed in this article to measure in two medium with very different RI such as PBS and whole blood. A third, simpler approach that provided a satisfactory result was to perform continuous measurement of the SPR curve intensity at the detection angle, which is obtained from the average intensity measured by the Si detector (DC component described in Fig. 1b schematics). The DC amplitude follows the development of the SPR curve (Fig. 6), which helps to eliminate nonspecific responses.

4. Conclusion

In this paper we proposed to combine the high sensitivity and multiplexing capability of eSPR method together with the high selectivity and robustness of structure-switching sensor in order to resolve several limitations of current biosensor for point-of-care applications. We did this by combining electrochemical and SPR characterization of a DNA-based structure-switching sensor that initiate spatial redox reporter displacement. This switch-based eSPR sensor displays a detection limit of 5 nM oligonucleotide and works as well in whole blood than in buffer. The multiplexing potential of this switch-based eSPR sensor was highlighted by simultaneous detection of two different oligonucleotide targets using two distinct nanoswitches attached to the same working electrode. This sensor supports the use of simplified planar electrodes for electrochemical scanning and can be implemented in a portable device arrangement with microfluidic and disposable sensing chips.

Acknowledgment

This work was funded by the Team Research Project of Fonds de recherche Nature et technologies (Québec, Canada) (Grant no. 2015-PR-183029). Anne-Marie Dallaire would like to thank the Natural Sciences and Engineering Research Council of Canada for the graduate scholarship. Alexis Vallée-Bélisle is a fellow from le Fond de Recherche en Santé du Québec and is the Canada Research Chair in Bio-engineering and Bio-nanotechnology.

References

Andersson, O., Ulrich, C., Bjorefors, F., Liedberg, B., 2008. Sens. Actuat. B – Chem. 134, 545–550.
Arinaga, K., Rant, U., Tornow, M., Fujita, S., Abstreiter, G., Yokoyama, N., 2006. Langmuir 22, 5560–5562.

Baba, A., Tian, S.J., Stefani, F., Xia, C.J., Wang, Z.H., Advincula, R.C., Johannsmann, D., Knoll, W., 2004. J. Electroanal. Chem. 562, 95–103.
Barik, A., Otto, L.M., Yoo, D., Jose, J., Johnson, T.W., Oh, S.H., 2014. Nano Lett. 14, 2006–2012.
Dahlin, A.B., Dielacher, B., Rajendran, P., Sugihara, K., Sannomiya, T., Zenobi-Wong, M., Voros, J., 2012a. Anal. Bioanal. Chem. 402, 1773–1784.
Dahlin, A.B., Zahn, R., Voros, J., 2012b. Nanoscale 4, 2339–2351.
Dallaire, A.M., Rioux, D., Rachkov, A., Patskovsky, S., Meunier, M., 2012. J. Phys. Chem. C 116, 11370–11377.
Fan, C.H., Plaxco, K.W., Heeger, A.J., 2003. Proc. Natl. Acad. Sci. USA 100, 9134–9137.
Gordon, J.G., Ernst, S., 1980. Surf. Sci. 101, 499–506.
Iwasaki, Y., Horiuchi, T., Morita, M., Niwa, O., 1998. Sens. Actuat. B – Chem. 50, 145–148.
Kang, X.F., Cheng, G.J., Dong, S.J., 2001. Electrochem. Commun. 3, 489–493.
Koetz, R., Kolb, D.M., Sass, J.K., 1977. Surf. Sci. 69, 359–364.
Liang, W.B., Wang, S.P., Festa, F., Wiktor, P., Wang, W., Magee, M., LaBaer, J., Tao, N.J., 2014. Anal. Chem. 86, 9860–9865.
Lu, J., Wang, W., Wang, S.P., Shan, X.N., Li, J.H., Tao, N.J., 2012. Anal. Chem. 84, 327–333.
Lubin, A.A., Lai, R.Y., Baker, B.R., Heeger, A.J., Plaxco, K.W., 2006. Anal. Chem. 78, 5671–5677.
Lubin, A.A., Plaxco, K.W., 2010. Acc. Chem. Res. 43, 496–505.
MacGriff, C., Wang, S.P., Wiktor, P., Wang, W., Shan, X.N., Tao, N.J., 2013. Anal. Chem. 85, 6682–6687.
Nakamoto, K., Kurita, R., Niwa, O., 2012. Anal. Chem. 84, 3187–3191.
Patskovsky, S., Latendresse, V., Dallaire, A.M., Dore-Mathieu, L., Meunier, M., 2014. Analyst 139, 596–602.
Rachkov, A., Patskovsky, S., Soldatkin, A., Meunier, M., 2011. Talanta 85, 2094–2099.
Reimhult, E., Larsson, C., Kasemo, B., Hook, F., 2004. Anal. Chem. 76, 7211–7220.
Rosi, N.L., Mirkin, C.A., 2005. Chem. Rev. 105, 1547–1562.
Rowe, A.A., White, R.J., Bonham, A.J., Plaxco, K.W., 2011. J. Vis. Exp. 52, 2922.
Sannomiya, T., Dermutz, H., Hafner, C., Voros, J., Dahlin, A.B., 2010. Langmuir 26, 7619–7626.
Scarano, S., Mascini, M., Turner, A.P.F., Minunni, M., 2010. Biosens. Bioelectron. 25, 957–966.
Shan, X.N., Patel, U., Wang, S.P., Iglesias, R., Tao, N.J., 2010. Science 327, 1363–1366.
Shan, X.N., Wang, S.P., Wang, W., Tao, N.J., 2011. Anal. Chem. 83, 7394–7399.
Swensen, J.S., Xiao, Y., Ferguson, B.S., Lubin, A.A., Lai, R.Y., Heeger, A.J., Plaxco, K.W., Soh, H.T., 2009. J. Am. Chem. Soc. 131, 4262–4266.
Uzawa, T., Cheng, R.R., White, R.J., Makarov, D.E., Plaxco, K.W., 2010. J. Am. Chem. Soc. 132, 16120–16126.
Vallee-Belisle, A., Plaxco, K.W., 2010. Curr. Opin. Struct. Biol. 20, 518–526.
Vallee-Belisle, A., Ricci, F., Plaxco, K.W., 2009. Proc. Natl. Acad. Sci. USA 106, 13802–13807.
Wain, A.J., Do, H.N.L., Mandal, H.S., Kraatz, H.B., Zhou, F.M., 2008. J. Phys. Chem. C 112, 14513–14519.
Wang, S.P., Huang, X.P., Shan, X.N., Foley, K.J., Tao, N.J., 2010. Anal. Chem. 82, 935–941.
Wang, W., Foley, K., Shan, X., Wang, S.P., Eaton, S., Nagaraj, V.J., Wiktor, P., Patel, U., Tao, N.J., 2011. Nat. Chem. 3, 249–255.
White, R.J., Plaxco, K.W., 2010. Anal. Chem. 82, 73–76.